MAGNETIC RESONANCE IN CHEMISTRY
*Magn. Reson. Chem.* 2004; **42**: 313–320
Published online in Wiley InterScience (www.interscience.wiley.com). DOI: 10.1002/mrc.1351

# Effects of polymorphic differences for sulfanilamide, as seen through $^{13}C$ and $^{15}N$ solid-state NMR, together with shielding calculations

**Alessia Portieri,[1] Robin K. Harris,[1]* (the late) Richard A. Fletton,[2] Robert W. Lancaster[2] and Terence L. Threlfall[3]**

[1] Chemistry Department, Durham University, South Road, Durham DH1 4LE, UK
[2] GlaxoSmithKline R & D Ltd, Medicines Research Centre, Gunnels Wood Road, Stevenage, Hertfordshire SG1 2NY, UK
[3] Department of Chemistry, University of Southampton, Southampton SO17 1BJ, UK

Received 29 August 2003; Accepted 06 November 2003

**We recorded both carbon-13 and nitrogen-15 NMR spectra of the three solid forms of sulfanilamide most commonly known. This study led to an interpretation of the solid-state effects seen in cross-polarization magic angle spinning spectra. Relaxation times for the different forms were measured. These show different behaviour for the three forms, arising from mobility variations. To obtain information on local environments, static spectra and spinning sideband manifolds were recorded and analysed for the $^{15}N$ resonances, using isotopically enriched samples. Shielding asymmetries and anisotropies for the two nitrogen nuclei were obtained, showing very different behaviour for the two sites. Shielding calculations were carried out for both $^{13}C$ and $^{15}N$ nuclei, and the results are discussed in relation to the experimental values. Copyright © 2004 John Wiley & Sons, Ltd.**

**KEYWORDS:** NMR; CP/MAS NMR; $^{13}C$ NMR; $^{15}N$ NMR; polymorphs; sulfanilamide; shielding computations; hydrogen bonding; relaxation

## INTRODUCTION

The term 'polymorphism' refers to the existence of different molecular packing arrangements of a given compound in the solid state.[1–3] The study of polymorphism and related solid-state phenomena has a long history, but has been given added impetus within the past decade, largely because of increasing awareness of its importance in the pharmaceutical industry. Unrecognized polymorphs, hydrates and amorphous forms, or unintended polymorphic transitions, can adversely affect the processing, stability and bioavailability of a drug substance in solid dosage forms.[4,5] Polymorphism and hydration have been associated with patent protection issues with major financial implications.[4]

Despite their importance, our ability to predict and sometimes even systematically prepare polymorphic crystal forms is limited.[6] The preparation and detection of polymorphs is therefore largely an empirical matter. Although many analytical methods can be used, often in complementary fashion,[1,7–10] solid-state NMR spectroscopy has been recognised as a major tool in the detection and quantification of polymorphs and in the study of polymorphism.[11,12] Its virtues include high discrimination between polymorphs, linked with molecular and intermolecular structural information.

In our laboratories, we have been studying in detail aspects of the solid-state behaviour of the sulfa drugs:

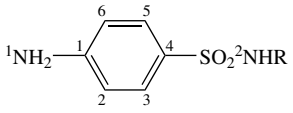


| | |
|---|---|
| R = H | sulfanilamide |
| R = 2-pyridyl, | sulfapyridine |
| R = 2-thiazolyl, | sulfathiazole |
| R = 2-pyrimidyl, | sulfadiazine |

These derivatives of sulfanilamide, which act as antibacterials, are extraordinarily versatile in their ability to crystallize in multiple solid-state structures. The polymorphic behaviour of the sulfa drugs has been repeatedly investigated[13–15] since their discovery in the late 1930s, but our recent studies have revealed unusual solid-state behaviour, new polymorphs and hundreds of solvates.[16,17]

Crystal structures of the three most accessible polymorphs of sulfanilamide itself ($\alpha$, $\beta$ and $\gamma$), obtained from single-crystal x-ray diffraction measurements, are to be found in the literature.[18–20] and can be retrieved from the Cambridge Crystal Structure Database. However, these data are relatively old and proved to be insufficiently accurate for our purposes, especially since they contain no information

*Correspondence to: Robin K. Harris, Chemistry Department, Durham University, South Road, Durham DH1 4LE, UK.
E-mail: r.k.harris@durham.ac.uk
Contract/grant sponsor: UK Engineering and Physical Sciences Research Council; Contract/grant number: GR/N05635.

about proton positions. We also used data obtained for one form by neutron diffraction experiments.[21] In addition, recent x-ray diffraction results for the three forms, of greater precision, have been obtained (M. J. Hursthouse and T. L. Threlfall, unpublished results; A. Portieri, R. K. Harris and H. Puschmann, unpublished results).

Other polymorphs (usually referred to as $\delta$-sulfanilamide) have been sporadically reported.[14,15,22] We have recently determined the crystal structure of a new polymorph, but have not been able to produce a sufficient quantity of pure material for spectroscopic characterization. Its calculated powder XRD pattern and stability indicate that it is not the $\delta$ polymorph reported by Sekiguchi *et al*.[14] An unstable anhydrate appears erratically during attempts to crystallize sulfanilamide polymorphs from aqueous solution. Its crystal structure has been reported.[23] The stability relationships between the polymorphs remain confused despite extensive investigation. The stable form at room temperature is $\beta$-sulfanilamide. All the other forms gradually revert to this on storage, although the lifetimes vary from sample to sample. On slow heating, $\beta$-sulfanilamide changes slowly to $\alpha$, which then transforms to $\gamma$, the highest melting form. Therefore, the $\gamma$ and $\beta$ forms must be enantiotropically related, but the situation in respect of $\alpha/\beta$ and $\alpha/\gamma$ is not clear. Burger[13] and Toscani and co-workers[24,25] reported the $\alpha$ and $\beta$ forms as monotropically related, but this is partly based on small melting enthalpy differences on samples of doubtful polymorphic purity. Sekiguchi *et al*.[14] suggested that they are enantiotropes with a transition point below room temperature. The usual (kinetic) transformation temperature recorded under typical differential scanning calorimetric heating rates is just above 100 °C. Our own work suggests a true transition temperature between 75 and 90 °C. The slow and variable transformation rates and the persistent formation of concomitant polymorphs[26] are the main reasons for the difficulty in determining the thermodynamic relationships.

In this paper, a detailed $^{13}C$ and $^{15}N$ solid-state NMR spectral study is presented of sulfanilamide and, in particular, of its three most accessible polymorphs: $\alpha$, $\beta$ and $\gamma$. Cross-polarization magic angle spinning (CP/MAS) $^{13}C$ NMR spectra of sulfanilamide have been presented previously,[27] although the assignment of some of the resonances was ambiguous because of the difficulties in crystallizing pure polymorphs, and also issues concerning the limited stability of the $\alpha$ form. Here we report a re-investigation of the $^{13}C$ NMR spectra of the sulfanilamide polymorphs, with a clarification of the assignments, aided by a study of the proton spin–lattice relaxation times in the laboratory and rotating frames, $T_1$(H) and $T_{1\rho}$(H), respectively. We also measured the high-resolution $^{15}N$ CP/MAS spectra of $^{15}N$-enriched samples for all the three solid forms for the first time. The value of $^{15}N$ spectra as an aid to the understanding of polymorphic behaviour has been shown previously in respect of dyestuffs[28,29] and pharmaceuticals.[30] In the present work, the separate enrichment of sulfanilamide at the N(1) and the N(2) positions allowed an insight into molecular mobility. The principal components of the nitrogen shielding tensors were also determined. Finally, Hartree–Fock (HF) and density functional theory (DFT) calculations of the shielding tensors of both $^{13}C$ and $^{15}N$ were carried out both for isolated molecules with the reported solid-state geometries and for molecular clusters. The effects of conformation and hydrogen-bonding patterns are discussed.

## EXPERIMENTAL

Commercial sulfanilamide was used for the $^{13}C$ NMR study, and the three forms were crystallized using literature techniques.[14,24] For the $\alpha$ form, about 500 mg of the sample were dissolved in 15 ml of *n*-butanol and the solution was heated to 90 °C and then cooled to ambient temperature. Long, needle-shaped crystals appeared when the residual solvent was left to evaporate overnight. For the $\beta$ form, about the same amount of sample was dissolved in water, which was then heated until the water evaporated to saturation conditions. Just after removing the solution to cool, crystals of the $\beta$ form started to crystallize. The $\gamma$ form was crystallized from ethanol. The solution was heated to about 80 °C and left to cool rapidly by positioning the flask in an ice-bath.

The isotopically enriched samples were synthesized by enriching in turn the two nitrogens of the molecule.

For the enrichment of N(2), the procedure followed was similar to that given in the literature[31,32] Thus, 12.5 ml of sulfonyl chloride were added to acetanilide (5 g) and left refluxing for about 1 h until no solid acetanilide was left. Ice was added to the solution, which was then filtered. A mixture of ammonium sulfate (Aldrich, 82.6% $^{15}N$; 9 mmol), the sulfonyl chloride acetanilide previously prepared (18 mmol) and $K_2CO_3$ (72 mmol) in acetonitrile (100 ml) was cooled in an ice-bath. Water (72 ml) was then added, the flask was stoppered and the mixture was stirred magnetically overnight. The organic layer was separated, the solvent was removed under vacuum and the residue was recrystallized from water. Then, following reflux with acid hydrolysis (2.5 ml of concentrated HCl and 7.5 ml of $H_2O$), the final product was obtained. Finally, the resulting sulfanilamide was crystallized in the different forms.

For the enrichment of N(1), 99%-enriched acetanilide (2 g) was purchased from Aldrich and $^{15}N$-enriched sulfonyl acetanilide was obtained as above. Ammonia was added to it, and the solution was heated for about 1 h. The hydrolysis and crystallization were carried out as above.

Carbon-13 CP/MAS spectra were obtained at ambient probe temperature (ca 298 K) using a Chemagnetics CMX 200 spectrometer operating at 50.329 MHz (corresponding to 200.13 MHz for protons). A two-channel Chemagnetics probe was used, with 7.5 mm o.d. 'pencil' rotors made of zirconia and Kel-F end-caps. The rotors contain about 350 mg of sample. Samples were packed into rotors without further grinding in order to minimize polymorphic changes. Operating conditions typically involved 5 μs 90° $^1H$ pulses and decoupling powers equivalent to 50 kHz. The recycle delay varied significantly, depending on the relaxation time of the particular form measured. A contact time of 1 ms was used for all forms and the spin rate was about 4 kHz. The experiments were carried out using different conditions for each polymorph. For $T_1$(H) measurements (via $^{13}C$ spectra

by pre-contact saturation-recovery) for the $\alpha$ and $\gamma$ forms, a recycle delay of 240 s was used and the recovery times were arrayed as 0.1, 5, 10, 20, 50, 80, 100, 120 and 150 s. The number of acquisitions per recovery time was 32. However, for the $\beta$ form spin–lattice relaxation time measurement, the recycle delay was 60 s, the number of transients was 32 and the recovery times were arrayed as 0.1, 1, 2, 3, 5, 8, 10, 12, 15, 20, 30 and 40 s. For $T_{1\rho}$(H), variable contact time experiments were performed by arraying 18 values: 0.1, 0.2, 0.4, 0.6, 0.8, 1, 1.2, 1.5, 2, 3, 4, 5, 6, 7, 8, 10, 12 and 15 ms. Recycle delays of 50 s were used for the $\beta$ form, but 200 s for the $\alpha$ and $\gamma$ forms.

Probe temperatures were calibrated based on the measurement of the frequency difference ($\Delta\nu$) between resonances for the methyl and hydroxyl protons of methanol in the $^1$H NMR spectrum of a sample of tetrakis(trimethylsilyl)silane soaked in liquid ethanol.[33] The $^{13}$C spectra were referenced to the signal for adamantane ($\delta_C = 38.4$ ppm from the TMS resonance for the high-frequency peak) by replacement. Detailed peak assignments were made using dipolar-dephased spectra,[34] which reveal resonances from quaternary carbons only.

Nitrogen-15 CP/MAS spectra at natural abundance were recorded using a Varian Unity Plus 300 spectrometer operating at 30.399 MHz. Spectra of the enriched samples were also recorded on the CMX 200 spectrometer and were obtained under approximately the same conditions as for the $^{13}$C measurements, but the 90° $^1$H pulse duration was 7 μs in this case, with typical contact times of 3 ms, and the referencing was obtained from a replacement sample of $^{15}NH_4NO_3$, with the nitrogen resonance from the nitrate group taken as $\delta_N = -5.1$ ppm (relative to the signal for nitromethane). Approximately 250 mg of sample were packed into the 5 mm outer diameter zirconia rotors (Kel-F caps) for the probe used.

The convention used herein for shielding parameters is that of Haeberlen.[35] The three tensor components are designated

$$|\sigma_{33} - \sigma_{iso}| \geq |\sigma_{11} - \sigma_{iso}| \geq |\sigma_{22} - \sigma_{iso}|$$

$$\text{Anisotropy } \zeta = \sigma_{33} - \sigma_{iso}$$

$$\text{Asymmetry } \eta = (\sigma_{22} - \sigma_{11})/\zeta$$

$$\text{Isotropic shielding } \sigma_{iso} = (\sigma_{11} + \sigma_{22} + \sigma_{33})/3$$

The sign convention means that the chemical shift, $\delta$, is $\sigma_{ref} - \sigma_{iso}$.

Spinning sideband analysis was carried out using both an in-house computer program,[36] ssb97, and STARS, supplied by Varian Associates, each based on the theory described by Maricq and Waugh.[37] The STARS program was also used to fit spectra of static samples.

For NMR shielding constant predictions, the Gaussian 94 program[38] was used for both HF and DFT methods, with basis sets such as 6–31G** or 6–311G** for carbon and D95** for nitrogen, all implemented with gauge-including atomic orbitals (GIAO). The calculations were taken to a high level of theory, namely triple zeta basis sets (6–311G**) and DFT methods such as B3PW91, which is a Becke[39] three-parameter functional with a Perdew–Wang gradient-correlated correction.[40] The geometries used were taken from both x-ray and neutron diffraction (ND) data. The computing facilities used were mainly those of the High Performance Computing Service at Durham University. This particularly involved a computer cluster by the name of hal, which consists of eight Sun Ultra 80 'nodes', each having four 450 Hz Ultra Sparc II processors with 2 Gbyte memory. The computed shielding values were converted to the chemical shift scale by subtracting the computed isotropic shielding constants of TMS (tetramethylsilane) (186.4 ppm)[41] for carbon and of nitromethane (−135.8 ppm)[42] for nitrogen.

## RESULTS AND DISCUSSION

In this work, we consider the crystal structures of the polymorphs in order to explore the relationship between the solid-state effects seen in the $^{13}$C and $^{15}$N spectra and structural variations. The main differences that are seen in the crystal structures (M. J. Hursthouse and T. L. Threlfall, unpublished results; A. Portieri, R. K. Harris and H. Puschmann, unpublished results) are associated with the dihedral angle, C(3)—C(4)—S(1)—N(2), as shown in Table 1. The signs in this table are defined as positive when the angle is clockwise as seen looking down at sulfanilamide from the amino group.

Proton relaxation times $T_1$(H) and $T_{1\rho}$(H) (in the rotating frame) for the three forms were measured by proton magnetization inversion–recovery and spin-locking respectively, followed by cross-polarization to carbon. These relaxation times proved to be very different at ambient probe temperature for the three polymorphs (see Table 2), indicating differences in molecular-level mobility.

Extensive variable-temperature measurements of $T_1$(H) and $T_{1\rho}$(H) were carried out for the $\beta$ form (only). It is not appropriate to discuss these in detail here, but suffice it to state that they showed evidence of at least two motional processes. Furthermore, the considerable variation in the

**Table 1.** Dihedral angles (°) for the various forms of sulfanilamide (M. J. Hursthouse and T. L. Threlfall, unpublished results; A. Portieri, R. K. Harris and H. Puschmann, unpublished results)

| Dihedral angle | $\alpha$ | $\beta$ | $\gamma$ | $\delta$ |
|---|---|---|---|---|
| C(3)—C(4)—S(1)—N(2) | 124.2 | 108.2 | 91.4 | 97.1 |
| C(5)—C(4)—S(1)—O(1) | 54.8 | 42.4 | 29.4 | 30.7 |
| C(3)—C(4)—S(1)—O(2) | 8.2 | −8.8 | −24.2 | −18.2 |

**Table 2.** Proton relaxation times, obtained via cross-polarization to $^{13}$C[a], for the three forms of sulfanilamide (at ca 298 K)

| Polymorph | $T_1$(H) (s) | $T_{1\rho}$(H) (ms) |
|---|---|---|
| $\alpha$ | 94 ± 4 | 7.2 ± 0.3 |
| $\beta$ | 8 ± 1 | 7.1 ± 0.1 |
| $\gamma$ | 82 ± 5 | 3.0 ± 0.1 |

[a] Values averaged over the different $^{13}$C signals are given and the errors quoted reflect the variations.

observed values helps to explain the significant differences between relaxation times for the different polymorphs at a single (ambient) temperature.

The ambient-temperature $T_1$ measurements allowed our experiments on $^{13}C$ spectra to be optimized and revealed to us that the first samples of the $\alpha$ polymorph which we examined were contaminated by the presence of the $\beta$ form. It is clear that if relatively short recycle delays are used in the cross-polarization experiment, then a small admixture of $\beta$ in a predominantly $\alpha$ sample will result in a spectrum with the $\beta$ peaks significantly enhanced. Conversely, a substantial impurity of $\alpha$ in $\beta$ may go undetected. Indeed, we believe that this problem was encountered in the work of Frydman *et al*.,[27] so that their results for the $\alpha$ form are probably suspect. Our optimized $^{13}C$ spectra of the three forms are illustrated in Fig. 1. Assignment of the signals can be made unequivocally, given the selection of quaternary carbon signals from dipolar dephasing experiments together with the known substituent effects on chemical shifts. The results (together with those of Frydman *et al*.[27]) are given in Table 3. Further assignment of the phenylene doublet C(2)/C(6) was feasible following shielding calculations, as these proved to predict the splitting, allowing us to assign C(2) [see Table 1 for the designation of C(3), which is bonded to C(2)] to the more shielded peak as seen from Table 5.

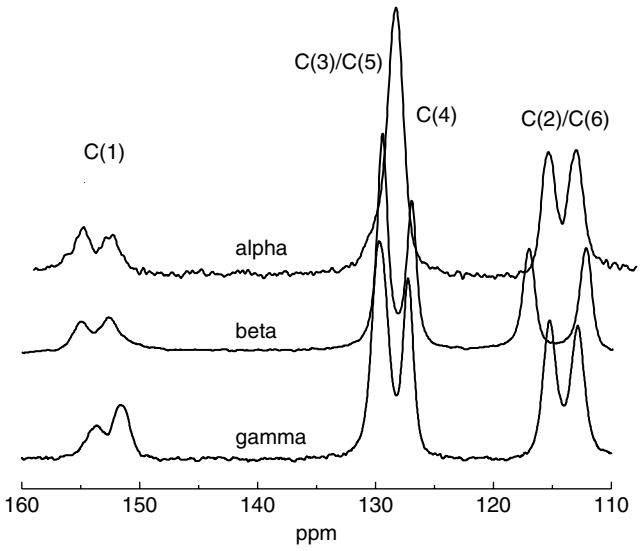


**Figure 1.** Carbon-13 CP/MAS spectra of the three forms of sulfanilamide.

There appear to be, consistently, differences in our chemical shifts from those of Frydman *et al*.,[27] possibly arising in part from differing practices of referencing (but also perhaps from different spectral quality). However, the absolute values are not the major point of interest. The C(1) signals are split into doublets because of residual (second-order) dipolar coupling arising from the quadrupolar nature of the directly bonded $^{14}N$ nuclei. A discussion of these splittings can be found in an earlier paper,[43] but we report in Table 3 only the weighted mean position of the signals (which is the true chemical shift), whereas Frydman *et al*.[27] quote the split peaks separately.

As can be seen, the major characteristic that distinguishes the three forms in the $^{13}C$ solid-state spectra is the splitting seen for resonances C(2)/C(6), an observation that is not clear in the paper of Frydman *et al*.[27] The values we obtain are 2.2, 4.8 and 2.4 ppm for the $\alpha$, $\beta$ and $\gamma$ forms, respectively. This splitting has been one of our major subjects of interest and, in this paper, we assign the origin to distortions of the amino group, which, as will be seen from $^{15}N$ relaxation times, is rigidly bonded to the phenylene ring.

Whereas raising the temperature for forms $\alpha$ and $\beta$ resulted in only minor variations of chemical shifts, the spectrum of the $\gamma$ form showed collapse of the C(2)/C(6) doublet above about 50 °C. Whereas this might arise from accidental shift equivalence at high temperature, it is more likely to stem from 180° phenylene ring flips, as was concluded by Frydman *et al*., who estimated the activation energy of this process to be ca 63 kJ mol$^{-1}$. It is concluded that the $\gamma$ polymorph exhibits more mobility than the other two forms.

Nitrogen-15 solid-state NMR spectra of the three forms showed significant differences in the isotropic chemical shifts only for N(2), as shown in Table 4. This shift seems to be greatly influenced by the dihedral angle of the sulfonamide group, since the smaller the angle the greater is the shielding. The fact that for N(1) the chemical shift is very similar in the solid and solution states is a sign of the small sensitivity to possible hydrogen bonds for this particular site in the molecule. This is confirmed from the crystal structure data, especially for the $\gamma$ form, in which this nitrogen does not participate in hydrogen bonding.

**Table 3.** Sulfanilamide $^{13}C$ chemical shifts (ppm) and assignments

| Polymorph | C(1) | C(4) | C(2) and C(6) | C(3) and C(5) |
|---|---|---|---|---|
| $\alpha$ (this work) | 153.7[a] | 128.0 | 113.1, 115.3 | 128.3 |
| $\alpha$ (Ref. 27)[b] | 166.5, 157.6 | 134.5 | 118.8, 124.0 | 134.5 |
| $\beta$ (this work) | 153.4[a] | 127.1 | 112.3, 117.1 | 129.5 |
| $\beta$ (Ref. 27) | 165.5, 156.0 | 135.6 | 118.3, 123.1 | 133.3 |
| $\gamma$ (this work) | 151.0[a] | 127.1 | 112.7, 115.1 | 129.6 |
| $\gamma$ (Ref. 27) | 165.1, 156.0 | 137.1 | 120.0, 122.5 | 135.0 |
| Solution in DMSO (Ref. 32) | 152.7 | 130.8 | 113.5 | 128.3 |

[a] The splitting magnitudes caused by residual dipolar coupling to $^{14}N$ are 131, 116 and 101 Hz for forms $\alpha$, $\beta$ and $\gamma$, respectively.

[b] Data for the $\alpha$ form from this source are suspect (see text).

**Table 4.** Isotropic chemical shifts, shielding anisotropies and asymmetries for nitrogen-15

| Polymorph | N(1) isotropic chemical shift (ppm) | N(2) isotropic chemical shift (ppm) | $\zeta$ for N(1) (ppm) | $\eta$ for N(1) | $\zeta$ for N(2) (ppm) | $\eta$ for N(2) |
|---|---|---|---|---|---|---|
| $\alpha$ | −312.2 | −288.8 | ±46 | 1 | 70.0 | 0.4 |
| $\beta$ | −312.1 | −284.1 | 43 | 0.8 | 71.2 | 0.4 |
| $\gamma$ | −312.1 | −280.6 | ±45 | 1 | 67.3 | 0.3 |
| Solution (DMSO)[a] | −312.4 | −284.0 | | | | |

[a] From Ref. 32.

One apparent oddity in the $^{15}$N spectra, which made work with natural abundance samples difficult, is that all three forms show an intense resonance for N(2), whereas only weak signals could be seen for N(1) at ambient probe temperature. Enriching the samples showed substantial differences in relaxation times for the two different nitrogen sites. For N(1) very long spin–lattice relaxation times (measured for $^{15}$N by the cross-polarization method[44]) of 100 s for the $\beta$ form and over 200 s for $\alpha$ and $\gamma$ (values which were, for obvious reasons, not very accurately measured) contrast with the relatively short relaxation times for N(2): 2.6 s for $\alpha$, 0.2 s for $\beta$ and 1.7 s for $\gamma$. Unlike the proton relaxation measurements, the nitrogen data can be assigned to local motions around the two different sites. They point clearly to significant differences in mobility in the region of the two nitrogens. Although the different values of $T_1$(N) cannot explain the differences in signal heights for the two $^{15}$N resonances directly, mobility effects can potentially influence $^{15}$N linewidths and lineshapes via interplay with MAS rates (and/or the decoupler power), perhaps giving the observed effects. The $^{15}$N relaxation behaviour was further investigated, although only for the $\beta$ form, through variable-temperature relaxation-time measurements. These experiments (Fig. 2) showed very different behaviour for the two sites and explain the fact that at ambient temperature $T_1$ for N(1) is nearly three orders of magnitude longer than that for N(2). In fact, the value for N(2) is very close to a minimum for 294 K (suggesting an energy barrier of ca 42 kJ mol$^{-1}$), whereas for N(1) it increases steeply as temperature decreases in that region, implying a significantly higher energy barrier to local motion. The value of $T_1$ for N(1) becomes much lower [ca 1 s, comparable to the ambient temperature value for N(2)] at higher temperatures, ca 380 K.

Values of $T_{1\rho}$($^{15}$N) were also measured for all three polymorphs at ambient probe temperature, using spin-lock powers equivalent to 50 kHz. For N(1) the value for the $\alpha$ and $\beta$ forms was 0.64 ms, whereas for the $\gamma$ polymorph it was 1.5 ms. Values for N(2) were significantly longer, namely 6.5, 10.0 and 4.2 ms, respectively, again pointing to substantially different mobility around the two sites.

We interpret the mobility of only one part of the molecule as the reason why we see a splitting in the $^{13}$C resonances for the *ortho* carbons only on the side of the amino group [C(2)/C(6)]. Mobility of the sulfonamide group might (at least partially) average the influence of this group on the carbons in the position *ortho* to it [i.e. C(3)/C(5)]. Small distortions of the amino group, on the other hand, would influence significantly the carbons C(2)/C(6) owing to its lack of mobility. The reason why the magnitude of the splitting

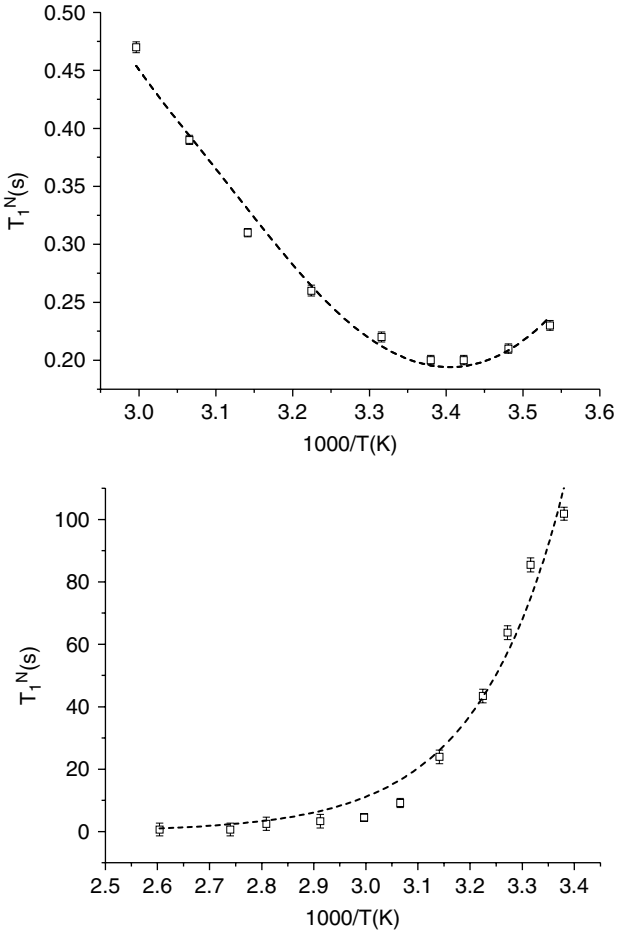


**Figure 2.** Variable-temperature spin–lattice relaxation times for $^{15}$N nuclei in the $\beta$ form: bottom, N(1); top, N(2).

for C(2)/C(6) for the $\beta$ form is greater than those for the other forms could be because this form has a significantly shorter C(1)—N(1) bond than in the other forms, showing a greater double-bond character: values for this bond-length (M. J. Hursthouse and T. L. Threlfall, unpublished results; A. Portieri, R. K. Harris and H. Puschmann, unpublished results) are 1.374 Å for the $\alpha$ form, 1.368 Å for the $\beta$ form and 1.377 Å for the $\gamma$ form.

For $^{15}$N, shielding anisotropies and asymmetries were measured for both the nitrogens of the molecule. Spinning sideband analysis was used for N(2), with the average values listed in Table 4. However, for N(1) it is not feasible to obtain an adequate number of resolved spinning sidebands for accurate analysis since the anisotropies are relatively small, so static spectra for N(1) were recorded and analysed instead,

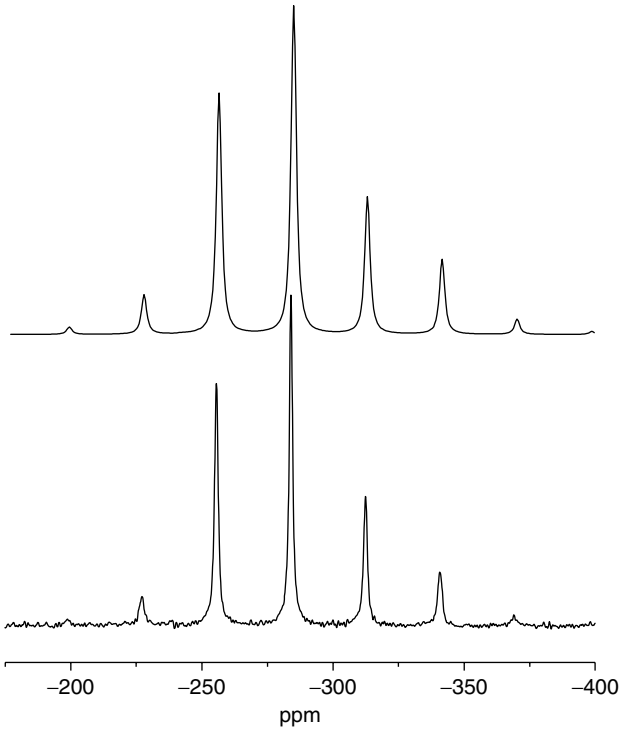


**Figure 3.** Nitrogen spectrum of the $\beta$ form for N(2): bottom, experimental; top, computer fitted. For the former, the spinning speed was 587 ± 3 Hz. The centreband is at −284.1 ppm.

with the results, which are of lower precision than those for N(2), shown in Table 4. An example of experimental and fitted spinning sideband manifolds for N(2) is illustrated in Fig. 3. Although the values of the anisotropies and asymmetries are different from one nitrogen to the other, there do not seem to be major differences from one form to another. The values for the asymmetries are near unity for N(1), making the sign of the anisotropy difficult to define.

## Computational procedures

The results of the computations of the isotropic $^{13}C$ chemical shifts for the isolated molecules with geometries as given in the crystal structures are listed and compared with the experimental data in Table 5. The shifts are clearly in the correct order, although errors in individual values are substantial in some cases.

Computations were also carried out for clusters of two, three or four molecules, corresponding to the arrangements in the crystal structures, in order to account for the effects of intermolecular interactions, particularly hydrogen bonding. Relevant contacts between heavy atoms below 3.11 Å were taken into account. For example, Fig. 4 shows the tetramer used for the $\alpha$-form computations. However, intermolecular effects were found to be relatively small. The most interesting aspect of the calculated results is that they are able to predict the splittings between carbons C(2)/C(6), which, when intermolecular effects are included, reach values near to the experimental data: 3.0 ppm for the $\alpha$ form, 4.9 ppm for the $\beta$ form and 3.3 ppm for the $\gamma$ form, to be compared with the experimental values of 2.2, 4.8 and 2.4 ppm, respectively. The results for the computations on the hydrogen-bonded clusters are shown in Table 6. The evidence of two distinct shielding constants for C(3)/C(5) is present in the calculations but not in the spectra, and this is presumably due to the fact that the sulfonamide group is fairly mobile so that the shielding values are averaged, as mentioned above. The best results were obtained when neutron diffraction data[21] were considered (available for only the $\beta$ form), indicating that the most important parameters required in order to obtain reasonably accurate shielding constants are precise hydrogen positions

**Table 6.** Computed isotropic chemical shifts for $^{13}C$ (in ppm) for hydrogen-bonded molecules, obtained using B3PW/6-311G** basis functions

| | $\alpha$ form | $\beta$ form | $\gamma$ form |
|---|---|---|---|
| C(4) | 132.9 | 133.8 | 133.5 |
| C(3) | 129.6 | 132.0 | 131.8 |
| C(2) | 109.6 | 112.5 | 108.9 |
| C(1) | 153.2 | 153.4 | 149.5 |
| C(6) | 112.6 | 117.4 | 112.2 |
| C(5) | 126.2 | 130.8 | 128.7 |
| R.m.s. | 2.9 | 3.2 | 3.8 |

**Table 5.** Experimental and calculated isotropic $^{13}C$ chemical shifts for the isolated molecules using the B3PW91/6−311G** model and single-crystal geometries derived from x-ray diffraction (M. J. Hursthouse and T. L. Threlfall, unpublished results; A. Portieri, R. K. Harris and H. Puschmann, unpublished results) and neutron diffraction data for the $\beta$ form

| | $\alpha$ form | | $\beta$ form | | $\gamma$ form | | $\beta$ form[a] | |
|---|---|---|---|---|---|---|---|---|
| Atom | Model | Expt. | Model | Expt. | Model | Expt. | Model | Expt. |
| C(4) | 136.1 | 128.0 | 135.9 | 127.1 | 135.8 | 127.1 | 134.6 | 127.1 |
| C(3) | 129.9 | 128.3 | 131.0 | 129.5 | 129.6 | 129.6 | 132.9 | 129.5 |
| C(2) | 108.3 | 113.1 | 110.3 | 112.3 | 107.1 | 112.7 | 110.1 | 112.3 |
| C(1) | 153.8 | 153.7 | 153.2 | 153.4 | 149.8 | 151.0 | 152.9 | 153.4 |
| C(6) | 109.7 | 115.3 | 111.1 | 117.1 | 110.0 | 115.1 | 114.5 | 117.1 |
| C(5) | 127.7 | 128.3 | 128.7 | 129.5 | 129.2 | 129.6 | 131.3 | 129.5 |
| R.m.s. error | 4.5 | | 4.5 | | 4.7 | | 3.7 | |

[a] Using geometry data from neutron diffraction results.[21]

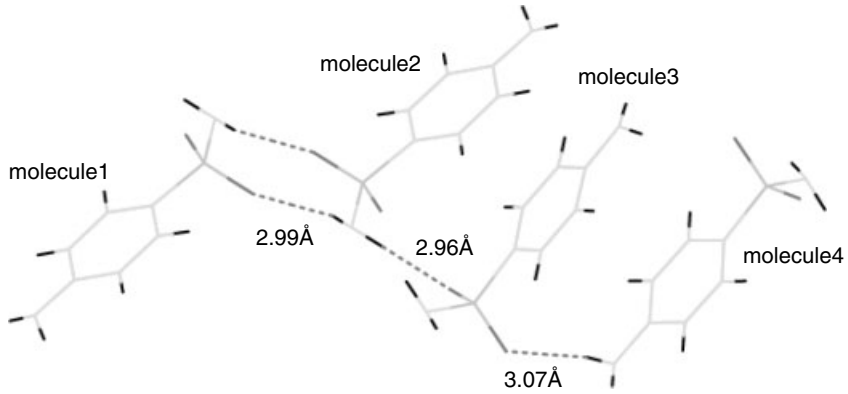


**Figure 4.** Tetramer used for the shielding calculations of the $\alpha$ form.

(see Table 5). Results using the neutron diffraction data show that the errors are not due to limitations of the basis sets but to imperfections of the positioning of the hydrogens.

Computations were also performed on $^{15}N$ shielding (Tables 7 and 8), and in this case the full tensor parameters were derived for comparison with the experimental results. Since $^{15}N$ is more sensitive to intermolecular effects, it proved to be important to include more than one molecule in the calculation; see Fig. 4. Including hydrogen bonds (two molecules per calculation, considering one hydrogen bond at a time), the differences between computed and observed $^{15}N$ isotropic chemical shifts (Table 7) become lower but they were still not completely satisfactory. For $^{15}N$ the reference calculation is clearly inadequate, as has been noted previously for theophylline.[30] Since the principal interest here lies in comparing data for the two nitrogens and for the different polymorphs, the values have been rebased by 37 ppm to facilitate such comparisons. In fact, the shift differences between N(1) and N(2) are well represented by the computations, whereas the variations between polymorphs appear to be too small to be accounted for by the theoretical results.

Results from the calculations of the full shielding tensors are shown in Table 8, where two molecules are considered for each computation. Since anisotropies and asymmetries are differences involving a single molecule, the computed values are expected to be more reliable than the absolute shieldings. Actually, the agreement between experimental and computed data is reasonable. However, in each case the experimental anisotropy is less than the computed value, presumably because of molecular motion. It is, though, surprising in this context that the experimental and theoretical ratios of the anisotropies for the two nitrogens in each form are similar.

**Table 8.** Comparison of calculated and experimental $^{15}N$ shielding anisotropies for the hydrogen-bonded molecules

| | Computed anisotropy | Computed asymmetry | Experimental anisotropy | Experimental asymmetry |
|---|---|---|---|---|
| $\alpha$(HB)— | | | | |
| $N(1)_{3.07\ \text{Å}}$ | −65 | 0.61 | ±46 | 1 |
| $N(2)_{2.99\ \text{Å}}$ | 83.9 | 0.48 | 70.0 | 0.4 |
| $N(2)_{2.96\ \text{Å}}$ | 86.1 | 0.47 | 70.0 | 0.4 |
| $\beta$ (HB)— | | | | |
| $N(1)_{3.03\ \text{Å}}$ | −51 | 0.8 | 43 | 0.8 |
| $N(2)_{3.10\ \text{Å}}$ | 83.2 | 0.47 | 71.2 | 0.4 |
| $N(2)_{3.00\ \text{Å}}$ | 86.9 | 0.44 | 71.2 | 0.4 |
| $\gamma$(HB)— | | | | |
| $N(2)_{3.00\ \text{Å}}$ | 83.2 | 0.50 | 67.3 | 0.3 |
| $N(2)_{3.01\ \text{Å}}$ | 82.1 | 0.51 | 67.3 | 0.3 |

**Table 7.** Experimental and calculated isotropic chemical shifts (in ppm) for N(1) and N(2)

| | Nitrogen[a] | B3LYP/D95** ($\sigma$) | Referenced ($\delta$) (−135.8 ppm) | Rebased by 37 ppm | Experimental ($\delta$) | Difference[b] |
|---|---|---|---|---|---|---|
| $\alpha$(HB) | $N(1)_{3.07\ \text{Å}}$ | 212.7 | −348.5 | −311.5 | −312.2 | 0.7 |
| | $N(2)_{2.99\ \text{Å}}$ | 188.3 | −324.1 | −287.1 | −288.8 | 1.7 |
| | $N(2)_{2.96\ \text{Å}}$ | 189.8 | −325.6 | −288.6 | −288.8 | 0.2 |
| $\beta$(HB) | $N(1)_{3.03\ \text{Å}}$ | 213.2 | −349.0 | −312.0 | −312.1 | 0.1 |
| | $N(2)_{3.00\ \text{Å}}$ | 188.1 | −323.9 | −286.9 | −284.1 | −2.8 |
| | $N(2)_{3.10\ \text{Å}}$ | 191.4 | −327.2 | −290.2 | −284.1 | −6.1 |
| $\gamma$(HB) | $N(2)_{3.00\ \text{Å}}$ | 182.4 | −318.2 | −281.2 | −280.6 | −0.6 |
| | $N(2)_{3.01\ \text{Å}}$ | 182.5 | −318.3 | −281.3 | −280.6 | −0.7 |

[a] The subscript is the H-bonded distance used for the computation.

[b] Computed minus experimental.

## CONCLUSIONS

We have shown here that the $\alpha$, $\beta$ and $\gamma$ forms of sulfanilamide may be clearly distinguished by their $^{13}C$ NMR spectra, but only if detailed attention is paid to the experimental conditions. This is especially important if mixtures of polymorphs are to be quantified. Moreover, it is important to combine data from $^{13}C$ and $^{15}N$ spectra in order to understand the mobility of the whole system. Further light has been thrown on the molecular-level behaviour of the polymorphs by relaxation time measurements and, in the case of $^{15}N$, by analyses of spinning sideband manifolds and of static spectra, yielding shielding tensor information. Computations of the shielding parameters using both isolated molecule and molecular cluster approaches have brought additional understanding of the differences between polymorphs in the splittings of the ortho-carbon resonances and in the ratio of $^{15}N$ shielding anisotropies.

### Acknowledgement

We thank the UK Engineering and Physical Sciences Research Council for support under grant GR/N05635. Robin K. Harris is grateful to the Leverhulme Trust for the award of an Emeritus Fellowship.

## REFERENCES

1. Threlfall TL. *Analyst* 1995; **120**: 2435.
2. Caira MR. *Top. Curr. Chem.* 1998; **198**: 163.
3. Yu L, Reutzel S, Stephenson G. *Pharm. Sci. Technol. Today* 1999; **1**: 118.
4. Bernstein J. *Polymorphism in Molecular Crystals*, Oxford University Press: Oxford, 2002.
5. Chemburkar SR, Bauer J, Deming K, Spiwek H, Patel K, Morris J, Henry R, Spanton S, Dziki W, Porter W, Quick J, Bauer P, Donaubauer J, Narayanan RA, Soldani M, Riley D, McFarland K. *Org. Proced. Res. Dev.* 2000; **4**: 413.
6. Gavezotti A. *Acc. Chem. Res.* 1994; **27**: 309.
7. Threlfall T. In *The Encyclopedia of Vibrational Spectroscopy*, Griffiths P, Chalmers J (eds). Wiley: Chichester, 2001; **5**: 3557–3573.
8. Szelagiewicz M, Marcolli C, Cianferani S, Hard AP, Vit A, Burkhard A, von Raumer M, Hofmeier U Ch, Zilian A, Francotte E, Schenker J. *Journal of Thermal Analysis and Calorimetry* 1999; **57**: 23.
9. Bernstein J. In *Industrial Applications of X-ray Diffraction*, Chung FH, Smith DK (eds). Marcel Dekker: New York, 2000; 21.
10. Giron D. *Thermochim. Acta* 1995; **248**: 1.
11. Christopher EA. PhD Thesis, University of Durham, 1993.
12. Bugay D. *Pharm. Res.* 1993; **10**: 317.
13. Burger A. *Sci. Pharm.* 1973; **41**: 290.
14. Sekiguchi K, Tsuda Y, Kanke M. *Chem. Pharm. Bull.* 1975; **23**: 1353.
15. Lin HO, Baenziger NC, Guillory JK. *J. Pharm Sci.* 1974; **63**: 145.
16. Apperley DC, Fletton RA, Harris RK, Lancaster RW, Taverner S, Threlfall TL. *J. Pharm. Sci.* 1999; **88**: 1275.
17. Bingham A, Hughes D, Hursthouse MB, Lancaster RW, Taverner S, Threlfall, TL. *Chem. Commun.* 2001; 601.
18. O'Connor BH, Maslen EN. *Acta Crystallogr.* 1965; **18**: 363.
19. Alléaume M, Decap J. *Acta Crystallogr.* 1965; **18**: 731.
20. Alléaume M, Decap J. *Acta Crystallogr.* 1965; **19**: 934.
21. O'Connell AM, Maslen EN. *Acta Crystallogr.*, 1967; **22**: 134.
22. McLachlan D. *X-ray Crystal structure*. McGraw-Hill: New York, 1957.
23. Alléaume M, Decap J. *Acta Crystallogr.* 1968; **24**: 214.
24. Toscani S, Thoren S, Agafonov V, Ceolin R, Dugue J. *Pharm. Res.* 1995; **12**: 1453.
25. Toscani S, Dzyabchenko A, Agafonov V, Dugue J, Ceolin R. *Pharm. Res.* 1996; **13**: 151.
26. Bernstein J, Davey RJ, Henck J-O. *Angew. Chem. Int. Ed. Engl.* 1999; **38**: 3440.
27. Frydman L, Olivieri AC, Diaz LE, Frydman B, Schmidt A, Vega S. *Mol. Phys.* 1990; **70**: 563.
28. McGeorge G, Harris RK, Chippendale AM, Bullock JF. *J. Chem. Soc., Perkin Trans. 2* 1996; 1733.
29. McGeorge G, Harris RK, Batsanov AS, Churakov AV, Chippendale AM, Bullock JF, Gan Z. *J. Phys. Chem. A* 1998; **102**: 3505.
30. Smith EDL, Hammond RB, Jones MT, Roberts KJ, Mitchell JBO, Price SL, Harris RK, Apperley DC, Cherryman JC, Docherty R. *J. Phys. Chem. B* 2001; **105**: 5818.
31. Ott DG. *Synthesis with Stable Isotopes of Carbon, Nitrogen and Oxygen*. Wiley; New York, 1981.
32. Pomerantz M, Chou W, Witczak MK, Smith CG. *J. Org. Chem.* 1987; **52**: 159.
33. Aliev AE, Harris KDM. *Magn. Reson. Chem.* 1994; **32**: 366.
34. Opella SJ, Frey MH. *J. Am. Chem. Soc.* 1979; **101**: 5854.
35. Haeberlen U. *Adv. Magn. Reson.* 1976; Suppl. 1: 9.
36. Ascenso JR, Merwin LH, Bai H-P, Cherryman JC, Harris RK. unpublished (originally mentioned in the open literature in Harris RK, Sebald A. *J. Organomet. Chem.* 1989; **85**: 1409).
37. Maricq MM, Waugh JS. *J. Chem. Phys.* 1979; **70**: 3300.
38. Frish MJ, Trucks GW, Schelegel HB, Scuseria GE, Robb MA, Cheeseman JR, Zakrzewsi VG, Montgomery JA, Stratman RE, Burant JC, Dapprich S, Millan JM, Daniels AD, Kudin KN, Strain MC, Farkas O, Tomasi J, Barone V, Cossi M, Cammi R, Mennucci B, Pomelli C, Adamo C, Clifford S, Ochtersky J, Petersson GA, Ayala PY, Cui Q, Morokuma K, Malick DK, Radbuck AD, Raghavachari K, Foresman JB, Cioslowsi J, Ortiz JV, Stefanov BB, Liu G, Liashenko A, Piskorz P, Komaromi I, Gomperts R, Martin RL, Fox DJ, Fox TA, Keith TA, Al-Laham MA, Peng CY, Nanayakkara A, Gonzalez C, Challcombe M, Gill PMW, Johnson BG, Chen W, Wong MW, Andres JL, Head-Gordon M, Replogle ES, Pople JA. *Gaussian 94, Revision C.2*. Gaussian: Pittsburgh, PA, 1995.
39. Becke AD. *J. Chem. Phys.* 1993; **98**: 5648; Becke AD. *J. Chem. Phys.* 1996; **104**: 1040.
40. Perdew JD, Burke K, Wang Y. *Phys. Rev. B* 1996; **54**: 16 533.
41. Jameson AK, Jameson CJ. *Chem. Phys. Lett.* 1987; **134**: 461.
42. Jameson CJ, Mason J. *Multinuclear NMR*. Plenum Press: New York, 1987.
43. Harris RK, Olivieri AC. *Prog. Nucl. Magn. Reson. Spectrosc.* 1992; **24**: 435.
44. Torchia DA. *J. Magn. Reson.* 1978; **30**: 613.